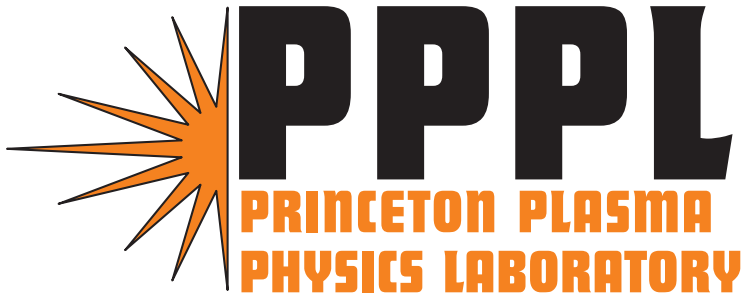

The vacuum Green's Function valid for high toroidal mode number in tokamaks New PEST results for NSTX*

– M. S. Chance and J. Manickam, (PPPL)

NSTX Results/Theory Review
Macroscopic Stability TSG
PPPL, Princeton, NJ, USA
September 15 – 16, 2009

*Work supported by U.S. Department of Energy Contract Nos. DE-AC02-76-CH03073 and DE-AC03-99ER54463.

Introduction: Motivation

- The previous evaluation of the Green's function in the VACUUM code relies on an upward recursion relation in n, initiated from the complete elliptic integrals of the first and second kinds.

$$\mathcal{G}^{n+1} = \frac{4n(2\hat{\rho}^2+1)}{(2n+1)}\mathcal{G}^n - \frac{2n-1}{2n+1}\mathcal{G}^{n-1}, \tag{1}$$

  for $n = 1, 2, \ldots$.

- Significant loss of digits occurs when studying moderately high n MHD modes. A few recursions in n can quickly lead to a complete loss of accuracy even when the seed elliptic integrals from [1] are replaced with the much more accurate recursive method of Bulirsch[4, 2].

- These inaccuracies have affected recent PEST applications on NSTX. The replacement of a more accurate calculation of $\mathcal{G}$[3] has resolved this.

The VACUUM code methodology: The response to the magnetic scalar potential, χ

The VACUUM code solves for the magnetic scalar potential, χ, as a response $\mathcal{C}$, to B_n, the normal component of the magnetic field at the plasma surface parameterized by $[X(\theta), Z(\theta)]$, $0 \leq \theta \leq 2\pi$ in a local coordinate system $(\mathcal{Z}, \theta, \phi)$. $\nabla\mathcal{Z}$ is normal to the surface with $\mathcal{J} = (\nabla\mathcal{Z} \times \nabla\theta \cdot \nabla\phi)^{-1}$.

Thus:

$$\chi_{l'}(\theta, \phi) = \sum_{l} \mathcal{C}_{l'l} \mathcal{B}^p_l e^{-in\phi}, \quad n \neq 0 \tag{2}$$

where $\mathcal{B}^p_l$ is the Fourier component of the normalized normal field, $\mathcal{B}^p(\theta) \equiv \mathcal{J}\nabla\chi \cdot \nabla\mathcal{Z}$

The response $\mathcal{C}_{ll'}$, a Hermitian matrix, contains the effects of the external boundary conditions.

$\mathcal{C}_{ll'}$ is calculated via the application of Green's second identity in which the defining functions are χ and the free space Green's function,

$$G(\mathbf{r}, \mathbf{r}') = \frac{1}{|\mathbf{r} - \mathbf{r}'|} \tag{3}$$

The two dimensional Green's function, $\mathcal{G}^n$

Fourier analyze in ϕ:

$$\mathcal{G}^n \equiv \frac{1}{2\pi}\oint \frac{e^{in(\phi-\phi')}}{|\mathbf{r}-\mathbf{r}'|}\,d\phi', \tag{4}$$

$$|\mathbf{r}-\mathbf{r}'|^2 = X^2 + X'^2 + (Z-Z')^2 - 2XX'\cos(\phi-\phi') \tag{5}$$

$$\mathcal{G}^n = \frac{1}{2\pi\sqrt{XX'}}\int_{-\pi/2}^{\pi/2} d\phi \frac{\cos 2n\phi}{\sqrt{\hat{\rho}^2+\sin^2\phi}}, \tag{6}$$

where $\hat{\rho}^2 = \rho^2/4XX'$, with $\rho^2 = (X-X')^2 + (Z-Z')^2$.

- $\mathcal{G}^n$ is a function of the two parameters, $\hat{\rho}$ and n.
- $\mathcal{G}^n$ is singular when $\hat{\rho} \longrightarrow 0$. The integrand oscillates for finite n and can lead to numerical difficulties.
- The accuracy of the method turns out to be dependent on the product, $n\hat{\rho}$. The old method breaks down at moderate $n\hat{\rho}$ and higher.

NSTX configuration

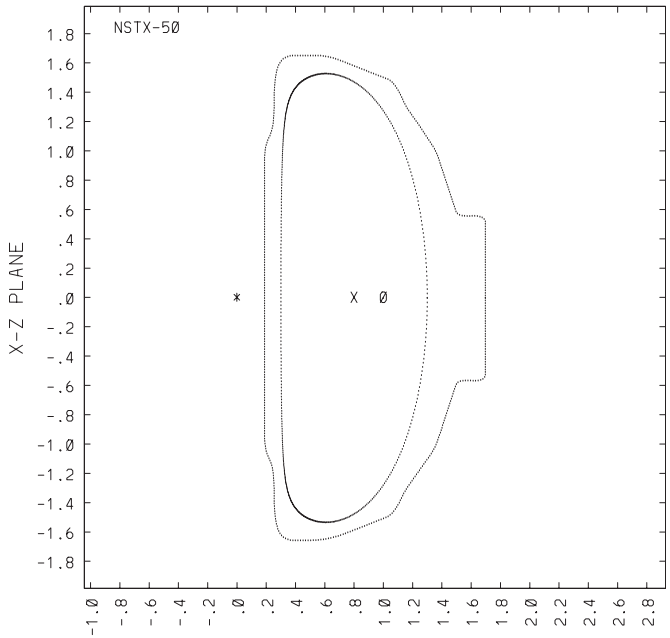

Plasma shape modeled from the record elongation shot of the Gates, et al. paper, Nucl. Fusion, 2007

Distance between source and observer:

$$\rho = \sqrt{(X - X')^2 + (Z - Z')^2}$$

$$\hat{\rho} = \rho / \sqrt{4 X X'}.$$

Example:

If $X \sim X' \sim 0.19$m, $Z - Z' \sim 3.0$m, then

$\hat{\rho} \sim 7.89$

Several alternatives to calculate $\mathcal{G}^n$

- More precise calculation of the seed elliptic integrals.
  - This only postpones the problem to higher n.
- Direct integration of Eq. (6) with due respect to its singular behavior.
  - Partially effective. Round off errors come into play beacuse of oscillations.
- Series expansion of the integrands
  - Partially effective. Limited range of validity. Good for checks.
  - New integral representation for $\mathcal{G}^n$ valid for moderate and large $n\hat{\rho}$.
    * Very effective. Complements the recursion method.

An alternative representation for $\mathcal{G}^n$

$$\mathcal{G}^n \equiv \frac{1}{2\pi}\oint \frac{e^{in(\phi-\phi')}}{|\mathbf{r}-\mathbf{r}'|}\,d\phi', \tag{7}$$

- Complex plane: $\phi \equiv u + iv$

$$\mathcal{G}^n = \frac{1}{2\pi\sqrt{XX'}}\mathcal{R}e\int_{-\pi/2}^{\pi/2}\frac{e^{2in\phi}\,d\phi}{\sqrt{\hat{\rho}^2+\sin^2\phi}}, \tag{8}$$

$$= \frac{1}{2\pi\sqrt{XX'}}\mathcal{R}e\int_{-\pi/2}^{\pi/2}\frac{e^{2in(u+iv)}\,d\phi}{\sqrt{\hat{\rho}^2+(\sin u\cosh v - i\cos u\sinh v)^2}}. \tag{9}$$

- For, $-\pi/2 < u < \pi/2$, the relevant branch points occur at $u = 0, v = \pm v_0$ where

$$v_0 = \sinh^{-1}\hat{\rho}. \tag{10}$$

Complex $\phi = u + iv$ plane

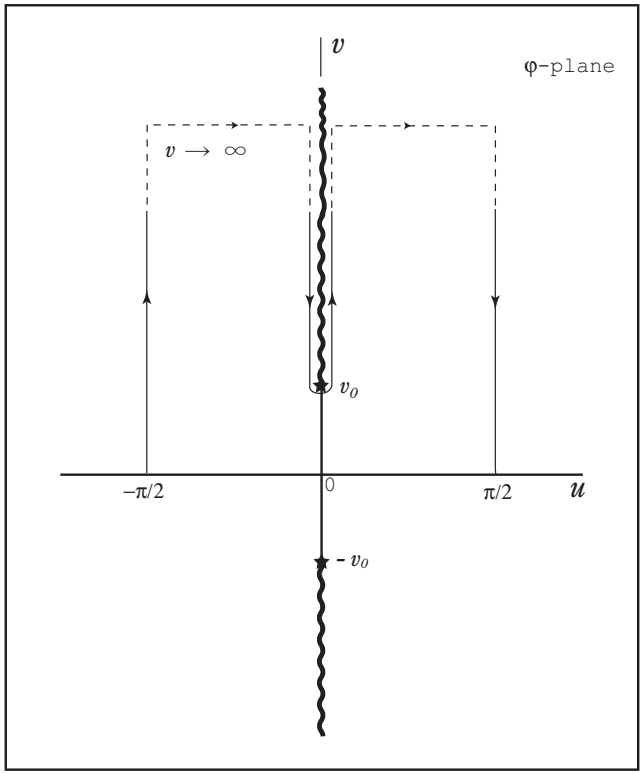

Figure 1: The complex $\phi = u + iv$ plane showing the branch points at $v_0 = \pm \sinh^{-1} \hat{\rho}$, the corresponding branch cuts denoted by the wavy lines, and the new deformed contour of integration which was originally along the real axis over the range $[-\pi/2, +\pi/2]$. The contributions along the segments $u = \pm\pi/2, 0 \leq v \leq \infty$ cancel each other, and there is no contribution from the branch point, so we are left with equal contributions from both sides of the branch cut along the positive imaginary axis,

New contour of integration

- The branch cuts are chosen as shown in Fig. 1.

$$\mathcal{G}^n = \frac{1}{\pi\sqrt{XX'}}\mathcal{R}e\int_{v_0}^{\infty}\frac{i\,e^{-2nv}\,dv}{\sqrt{\hat{\rho}^2-\sinh^2 v}}. \tag{11}$$

- Let $v \equiv v_0 + z/2n$:

$$\mathcal{G}^n = \frac{e^{-2nv_0}}{2n\pi\sqrt{XX'}}\int_0^{\infty}\frac{e^{-z}\,dz}{\sqrt{\sinh^2(v_0+z/2n)-\hat{\rho}^2}}, \tag{12}$$

$$= \frac{e^{-2nv_0}}{2n\pi\sqrt{XX'}}\int_0^{\infty}\frac{e^{-z}\,dz}{\sqrt{(2\hat{\rho}^2+1)\sinh^2(z/2n)+\hat{\rho}(\hat{\rho}^2+1)^{1/2}\sinh(z/n)}}, \tag{13}$$

- The integrand is non-oscillatory and positive definite leaving the result of the cancellations when $n\hat{\rho}$ is large, in the exponential factor, e^{-2nv_0}. Actually a demonstration of the Riemann-Lebesgue lemma for this integral.

Gaussian Quadratures

- Can numerically evaluate the integral Eq. (13)
- Introduce another change of variable, $z = t^2$

$$\mathcal{G}^n = \frac{\sqrt{2}\, e^{-2nv_0}}{n\pi\sqrt{XX'A}} \int_0^\infty \frac{t\, e^{-t^2} dt}{\sqrt{2B\sinh^2(t^2/2n) + \sinh(t^2/n)}}. \tag{14}$$

$$A \equiv 2\hat{\rho}\sqrt{\hat{\rho}^2+1}, \qquad B \equiv \frac{2\hat{\rho}^2+1}{2\hat{\rho}\sqrt{\hat{\rho}^2+1)}}, \tag{15}$$

- Integrand is well behaved for $\hat{\rho} \neq 0$ and amenable to Gaussian quadratures.
- Because of the strong Gaussian decay of the integrand, sufficient accuracy is obtainable if the range of integration is finite.
- Results checked by comparison with trapezoidal and expansion methods.

Constant relative error

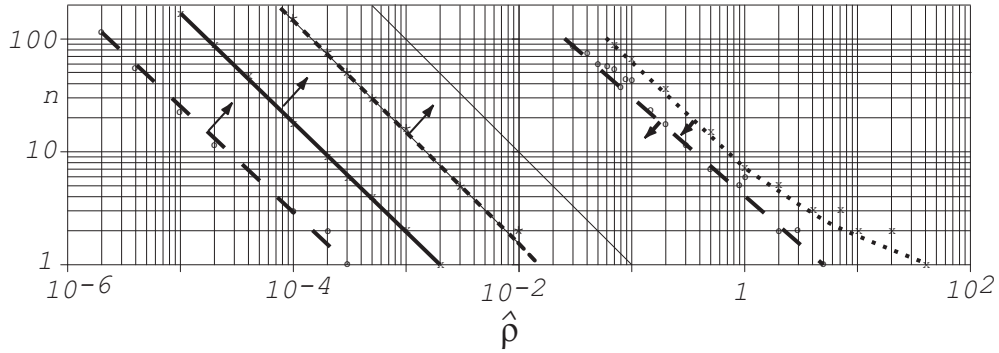

Constant relative error, ε, in the n vs. $\hat{\rho}$ plane over eight orders of magnitude in $\hat{\rho}$. The three straight lines on the left show the results using Gaussian integration of Eq. (14). Dashed line: $\varepsilon = 10^{-6}$ with 64 points over the range [0,7]. Thick solid line: $\varepsilon = 10^{-9}$ using 64 points in [0,7] and also closely represents $\varepsilon = 10^{-6}$ using 32 points in [0,5]. Dotted line: $\varepsilon = 10^{-9}$ using 32 points in [0,5]. The two lines on the right correspond to $\varepsilon = 10^{-9}$, for the trapezoidal (dotted line) and recursion (dashed line) methods. The arrows indicate the direction where the relative error decreases. The thin solid line coresponds to $n\hat{\rho} = 10^{-1}$

Choose old method for $n\hat{\rho} \leq 0.1$ and new method otherwise.

Asymmetry the response matrix, $\mathcal{C}_{ll'}$

$\mathcal{C}_{ll'}$ should be Hermitian:

```
                    JOBID = nstx-50

                 Asymmetries in the response

                ----------------------

Sum of diagonals, sd =                2.8714E+06

Sum of off-diagonals, sod =           5.1338E+06

Difference in off diagonals, dod =    4.7385E+00


Asymmetry [dod/sod] =                 9.2301E-07

          [dod/(sd+sod)] =            5.9193E-07

                                     ------------
```

Comparison between old and new

Asymmetry, dod/sod

n	Old	New
1	4.9002E-06	4.9177E-06
3	3.5421E-05	1.4772E-06
5	5.4379E-02	9.2401E-07
10	7.2024E-01	3.7150E-07
15	7.6367E-01	2.6245E-07
20	xxxx	2.4956E-07
50	xxxx	5.9193E-07
...	xxxx	...

- Old method breaks down even at $n = 5$
- New method still accurate at $n = 50$ and beyond.

PEST-II results on NSTX – I

The modified PESTcode now correctly calculates that the most unstable toroidal mode number for the NSTX shot 129015 is $n = 4$. Previous calculations broke down at $n \sim 2 - 3$.

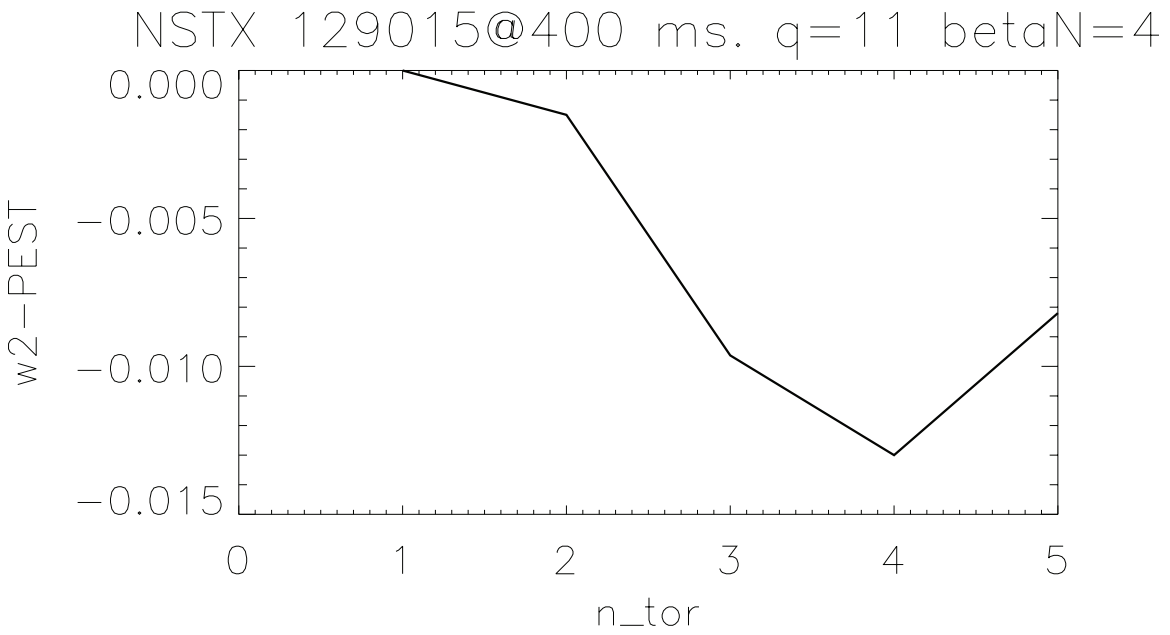

PEST-II results on NSTX – II

Some preliminary calculations to study the shape dependence on ELMS stability for moderately high n in NSTX. This is relevant to the XP proposed by Aaron Sonntag.

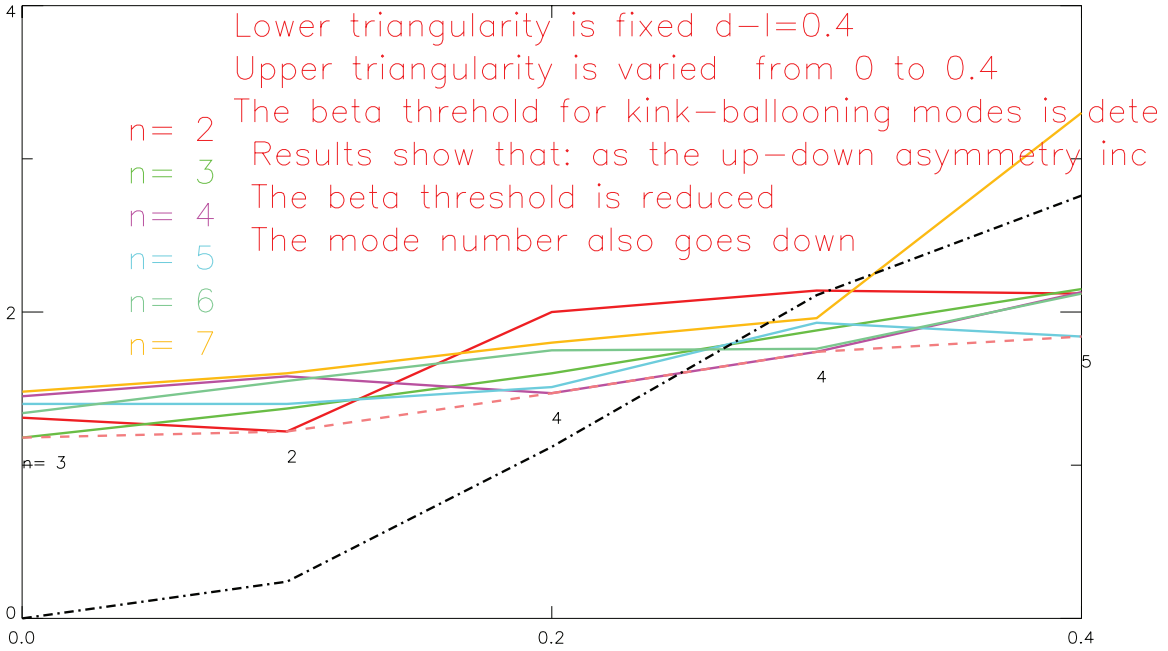

Relationship to the Legendre polynomials

- An integral representation of the associated Legendre function as a function of its conventional variable s, which has its origins in spherical coordinates:

$$P_\nu^n(s) = \frac{\Gamma(\nu+n+1)}{2\pi\Gamma(\nu+1)} \oint \left[s + \sqrt{s^2-1}\cos\phi\right]^\nu e^{in\phi}\, d\phi. \tag{16}$$

$$s = \frac{2\hat{\rho}^2+1}{2\sqrt{\hat{\rho}^2(\hat{\rho}^2+1)}} = \frac{2\hat{\rho}^2+1}{2\hat{\mathcal{R}}^2} \tag{17}$$

$$\text{where} \quad \mathcal{R}^2 = 4XX'\sqrt{\hat{\rho}^2(\hat{\rho}^2+1)} \equiv 4XX'\hat{\mathcal{R}}^2. \tag{18}$$

$$\mathcal{G}^n = \frac{\Gamma(1/2-n)}{\pi^{1/2}\mathcal{R}} P^n_{-1/2}(s), \tag{19}$$

New representation for the Legendre function

- Use Eqs. (14) and (19) to find:

$$P^n_{-1/2}(s) \;=\; \frac{1}{\sqrt{\pi}\Gamma(1/2-n)}\left(\frac{s-1}{s+1}\right)^{n/2}\int_0^\infty \frac{e^{-nt}\,dt}{\sqrt{2s\sinh^2(t/2)+\sinh t}}. \qquad (20)$$

- Generalize to arbitrary ν but $\nu > -1$:

$$P^n_\nu(s) \;=\; \frac{1}{\Gamma(\nu+1)\Gamma(-\nu-n)}\left(\frac{s-1}{s+1}\right)^{n/2}\times \int_0^\infty \left[2s\sinh^2(t/2)+\sinh t\right]^\nu e^{-nt}\,dt. \qquad (21)$$

- This constitutes a new integral representation of the associated Legendre polynomial of the first kind and properly reduces to that found in Eq. (20) when $\nu = -1/2$.

References

[1] Milton Abramovitz and Irene A. Stegun. *Handbook of Mathematical Functions*. Number 55 in Applied Mathematics Series. National Bureau of Standards, Superintendent of Documents, U.S. Goverment Printing Office, Washington, D.C. 20402, ninth edition, November 1970.

[2] Roland Bulirsch. Numerical calculation of elliptic integrals and elliptic functions. *Numerische Mathematik*, 7(1):78–90, feb 1965.

[3] M. S. Chance, A. D. Turnbull, and P. B. Snyder. Calculation of the vacuum green's function valid even for high toroidal mode numbers in tokamaks. *jcp*, 221(1):330–448, jan 2007.

[4] W. H. Press, S. A. Teukolsky, W. T. Vetterling, and B. P. Flannery. *Numerical Recipes in Fortran 77: The Art of Scientific and Parallel Computing*. Cambridge University Press, 1996.